Temporal Characterization of the Functional Density of the Vasa Vasorum by Contrast-Enhanced Ultrasonography Maximum Intensity Projection Imaging

Sang Chol Lee, MD,*† Chad L. Carr, MD,* Brian P. Davidson, MD,*
Dilantha Ellegala, MD,* Aris Xie, MS,* Azzdine Ammi, PhD,* Todd Belcik, BS, RDCS,*
Jonathan R. Lindner, MD*

Portland, Oregon; and Seoul, South Korea

OBJECTIVES We sought to determine whether contrast-enhanced ultrasound (CEU) microangiography with maximum intensity projection (MIP) processing could temporally evaluate proliferation of the vasa vasorum (VV) in a model of mural hemorrhage.

BACKGROUND Expansion of the VV and plaque neovascularization contributes to plaque growth and instability and may be triggered by a variety of stimuli, including vascular hemorrhage. However, quantitative in vivo methods for temporal assessment of VV remodeling are lacking.

METHODS In 24 rabbits fed a high-fat diet, either autologous whole blood or saline was percutaneously injected into the media-adventitia of the femoral artery using ultrahigh-frequency ultrasound guidance. Functional VV density at the injection site and contralateral control artery was assessed 1, 2, and 6 weeks after injection with CEU imaging with MIP processing. In vitro studies with renathane microtubes were also performed to validate linear density measurement with CEU and MIP processing.

RESULTS In vitro studies demonstrated that MIP processing of CEU data reflected the relative linear density of vessels in a manner that was relatively independent of contrast concentration or microtube flow rate. On CEU with MIP, there was a 3-fold increase in femoral artery VV microvascular density at 1 and 2 weeks after blood injection (p < 0.01 vs. contralateral control), whereas VV density increased minimally after saline injection. At 6 weeks, VV vascular density decreased in blood-treated vessels and was not different from saline-injected or contralateral control vessels.

CONCLUSIONS CEU with MIP processing can provide quantitative data on temporal changes in the functional density of the VV. This method may be useful for evaluating high-risk features of plaque neovascularization or response to therapies aimed at plaque neovessels.   (J Am Coll Cardiol Img 2010; 3:1265–72) © 2010 by the American College of Cardiology Foundation

n atherosclerotic disease, expansion of the vasa vasorum (VV) and development of plaque neovessels that penetrate the tunica media and neointima have been causatively linked with lesion growth, expansion of the necrotic core, and plaque rupture (1–4). Plaque neovessels may promote plaque instability by serving as a portal of entry for immune cells, lipoproteins, and erythrocytes that contribute to the cholesterol pool and inflammatory milieu (1–4). The factors that initiate

See page 1273

VV remodeling include hypoxia and proangiogenic cytokines and growth factors produced as part of the inflammatory response (2–5). Plaque hemorrhage can also potentiate angiogenesis either directly or secondarily from stimulation of an inflammatory response (3,6), which could explain the association between occult plaque hemorrhage detected by angioscopy or magnetic resonance imaging with a future increase in lesion size and lipid content (7–9).

Noninvasive detection of the presence or therapeutic regression of VV or plaque neovessels relies on the ability to image mural microvascular density with high resolution and high sensitivity. Contrast-enhanced ultrasound (CEU) was used previously to detect plaque neovascularization in the carotid artery (10–13), although analysis methods have been qualitative and subject to influence by contrast concentration in the blood pool. In this study, we hypothesized that CEU with maximum intensity projection (MIP) processing could be used to temporally quantify changes in the functional VV density caused by mural hemorrhage.

ABBREVIATIONS AND ACRONYMS

CEU = contrast-enhanced ultrasound

MIP = maximum intensity projection

VV = vasa vasorum

MIP processing was used to optimize sensitivity for evaluating the VV under baseline and stimulated conditions and to provide a method for evaluating blood volume that is relatively independent of microbubble dose or concentration.

METHODS

Animal models of intramural hemorrhage. The study protocol was approved by the Animal Care and Use Committee at Oregon Health & Science University. Pilot experiments were performed to confirm that exposure to whole blood could stimulate VV proliferation in the femoral artery. Sprague-Dawley rats (250 to 300 g) were anesthetized with an intraperitoneal injection of ketamine hydrochloride (40 mg/kg), xylazine (8 mg/kg), and atropine (0.02 mg/kg). A sterile latex pouch 1 cm in length was placed around a femoral artery and its open edges were sealed with cyanoacrylate glue. Either autologous blood or sterile saline (100 μl, n = 3 for each) was injected into the cuff. Vessels were harvested for histology 10 days later.

For in vivo imaging of VV proliferation, 24 New Zealand white rabbits 3 to 4 months old were placed on a high-fat diet consisting of 1% cholesterol and 6% peanut oil. Two weeks after initiation of the high-fat diet, rabbits were randomized to receive femoral artery intramural injections (30 μl) of either autologous venous blood in sodium citrate or control saline injection. Animals were anesthetized and injections, into the adventitia and media of the near wall through a short-bevel 35-gauge needle were guided by a micromanipulation-microinjection system and ultrahigh frequency (55 MHz; beam elevation <1 mm) ultrasound imaging (Vevo 770, VisualSonics Inc., Toronto, Ontario, Canada) (Fig. 1, Online Videos 1
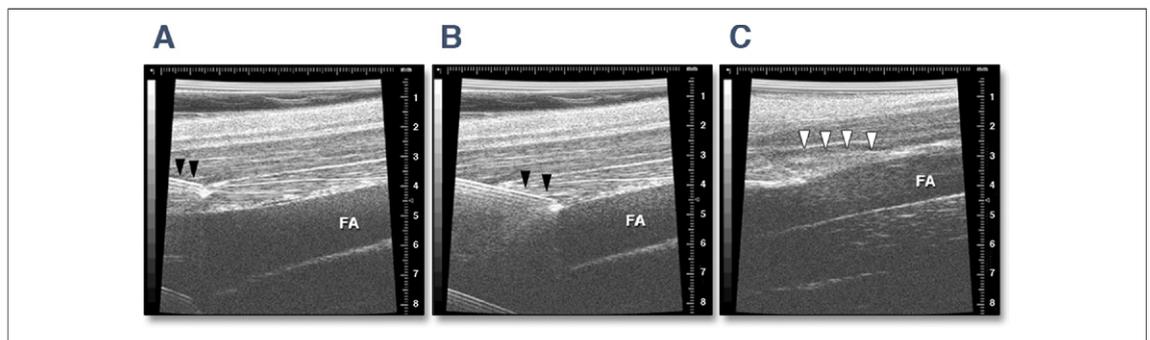
Figure 1. Percutaneous Intramural Microinjection of the Femoral Artery

(A, B) Images illustrating advancement of the short-bevel needle (**black arrowheads**) under ultrahigh frequency ultrasound (55 MHz) guidance to the near-wall of the femoral artery (FA). **(C)** Post-injection image showing injectate in the vessel wall (**white arrowheads**). See Online Videos 1 and 2 for illustrations of the positioning of the needle and real-time spatial distribution of the injectate.

and 2). Injections were made 5 mm proximal to the bifurcation of superficial and deep femoral arteries to provide an anatomic landmark for follow-up studies. A 5-mm longitudinal extension of the injectate typically occurred on either side of the injection site. A CEU study of the injected and contralateral control femoral artery was performed 1, 2, and 6 weeks after injection. An inflammatory response to hemorrhage in the rabbit model was assessed by CEU molecular imaging for intercellular adhesion molecule (ICAM)-1 and histology 48 h after injection.

VV imaging. Functional VV in the injected and the contralateral control femoral arteries was assessed using CEU and MIP processing (Aplio, Toshiba Medical Systems, Tohigi, Japan), which displays pixel intensity according to the maximum achieved after a destructive pulse sequence so that microbubbles leave a "trail of enhancement" during their transit (14). This method has been previously used to image functional microvascular density in angiogenic beds (14). Imaging (mechanical index 0.1) was performed in the longitudinal axis with a linear-array transducer. Imaging was performed at 7 MHz with a contrast-specific, low-power pulse-subtraction imaging.

Lipid-shelled decafluorobutane microbubbles were prepared by sonication of a gas-saturated aqueous suspension of 2 mg·ml^{-1} distearoylphosphatidylcholine and 1 mg·ml^{-1} polyoxyethylene-40-stearate. Microbubbles (5×10^7) were intravenously injected for 2 s. On full opacification of the vascular lumen (5 to 10 s after injection), MIP image sets were acquired after a 3-frame high-mechanical index destructive pulse sequence. Acquisitions were performed in triplicate for each artery. Mural microvascular density in the femoral artery was measured using quantitative pixel intensity threshold analysis, which determines the number or percentage of pixels in a region of interest that exceeds 10% of the average background (pre-contrast) videointensity, which generally represents >3 SD above mean background (15). Data were analyzed from frames obtained 2 s after the destructive pulse sequence using regions of interest placed over the femoral artery wall that extended 2 mm away from the lumen and that spanned 10 mm on either side of the injection site.

Evaluation of beam volume. The power spectrum of the acoustic beam from the transducer used for VV imaging was characterized to determine the volume of tissue imaged. A polyvinylidene fluoride needle hydrophone (Precision Acoustics, Dorchester, United Kingdom) was placed in a degassed water bath in line with the ultrasound transducer at a 1-cm separating distance. The hydrophone was interfaced with a pre-amplifier (HP1, Precision Acoustics) and oscilloscope (WaveRunner 44MXi-A, LeCroy Corp., Chestnut Ridge, New York). A total of 100 acoustic pressure waveforms were averaged from each position, which was adjusted in 50-μm adjustments in position in the elevational direction using an automated stepping motor controller (VXM, Velmex, Bloomfield, New York).

Molecular imaging. For molecular imaging of the inflammatory response, biotinylated hamster monoclonal IgG$_1$ against ICAM-1 (3E2, BD Pharmingen, San Diego, California) or control nonspecific IgG$_1$ were conjugated to the surface of microbubbles that contain a bifunctional molecule with a membrane anchoring domain and streptavidin at the end of a molecular spacer (MicroMarker-3, VisualSonics Inc.). CEU molecular imaging of the femoral artery in long-axis was performed in anesthetized rabbits with a linear-array probe (Sequoia, Siemens Medical Systems, Mountain View, California). The nonlinear fundamental signal component for microbubbles was detected with a multipulse protocol at a frequency of 7 MHz and a mechanical index of 1.0. Protocols were performed as previously described to detect the signal only from retained agent (16). Intensity was measured from a region of interest placed on the near wall of the artery extending 1.0 cm on either side of the injection site.

Histology. For immunohistology, perfusion fixation was performed by cannulation of the descending aorta. The femoral artery was removed together with surrounding connective tissue. Immunohistochemistry in the rat femoral artery was performed with a primary antibody against CD31 (3A12) and secondary antibody detection with 3,3′-diaminobenzidine chromagen. VV density was assessed by counting the number of CD31-positive vessels in the adventitia extending up to 200 μm from the media border. Hematoxylin and eosin staining was used to evaluate the inflammatory response 48 h after blood injection in rabbits. Immunostaining of CD31 in rabbits was unsuccessful despite attempts with several different primary antibodies.

In vitro validation of vascular density measurement. Acoustically transparent microrenathane tubes with an inner diameter of 120 mm (BrainTree Scientific Inc., Braintree, Massachusetts) were placed at a 30° incident angle to the ultrasound sector. Microbubble suspensions were infused through the tubing at a constant rate. Imaging parameters were identical to those of in vivo

studies and CEU data with MIP processing were collected for 2 s after a destructive pulse sequence. The following interacting variables were studied: 1) number of microvessels placed in the beam (n = 1 to 4); 2) microbubble concentration (range 1×10^5 to 5×10^6 ml^{-1}); and 3) flow rate through each tube (10 to 15 μl/s). Data were expressed as the number of pixels enhancing >3 SD beyond mean background signal.

Statistical analysis. Data were analyzed using RS/1 (version 6.0.1, Domain Manufacturing Corp., Burlington, Massachusetts). Comparisons of groups with regard to VV density and molecular imaging data were made using the Mann-Whitney rank-sum test. A Bonferroni procedure was used to correct for multiple comparisons according to treatment group. Changes in the same subject according to post-injection interval were compared using either Wilcoxon signed-rank test or a paired *t* test depending on whether data were distributed normally. Difference was considered significant at a p < 0.05.

RESULTS

In vitro experiments. In this study, MIP processing was used to detect the presence of microvessels that may have infrequent flux of microbubble contrast agent. In vitro flow studies with renathane microtubes were performed to determine whether the area with enhancement on MIP accurately depicts the linear density of microvessels. The sequential addition of microtubes in the ultrasound field resulted in a proportional increase in the area of enhancement across a clinically relevant range of microbubble concentrations (Fig. 2A). Despite a 50-fold increase from the lowest (1×10^5 ml^{-1}) to highest (5×10^6 ml^{-1}) microbubble concentration, there was only a small (<2-fold) difference in the area of enhancement. Across the full range of linear densities, a 50% increase in flow rate through each microtube resulted in a minimal (8 ± 2%) increase in the area of enhancement (Fig. 2B). In aggregate, these data imply that MIP enhancement area accurately depicts functional microvessel density in a manner that is not substantially influenced by microbubble concentration or flow rate.

Characterization of the ultrasound sector. The acoustic pressure profile in the ultrasound beam was characterized to determine the volume of tissue imaged when assessing VV density (Fig. 3). Assuming a 200-kPa peak negative acoustic pressure threshold for microbubble signal detection at 7 MHz (17), the effective elevational dimension was determined to be 1.8 mm. The rabbit femoral artery diameter was approximately the same (range 1.7 to 2.1 mm), indicating that most of the near wall volume was averaged into the 2-dimensional ultrasound display.

Blood-induced VV proliferation. Because of difficulties with CD31 staining in rabbits, the rat femoral artery was used for immunohistology evaluation of the VV response to blood exposure. Adventitial
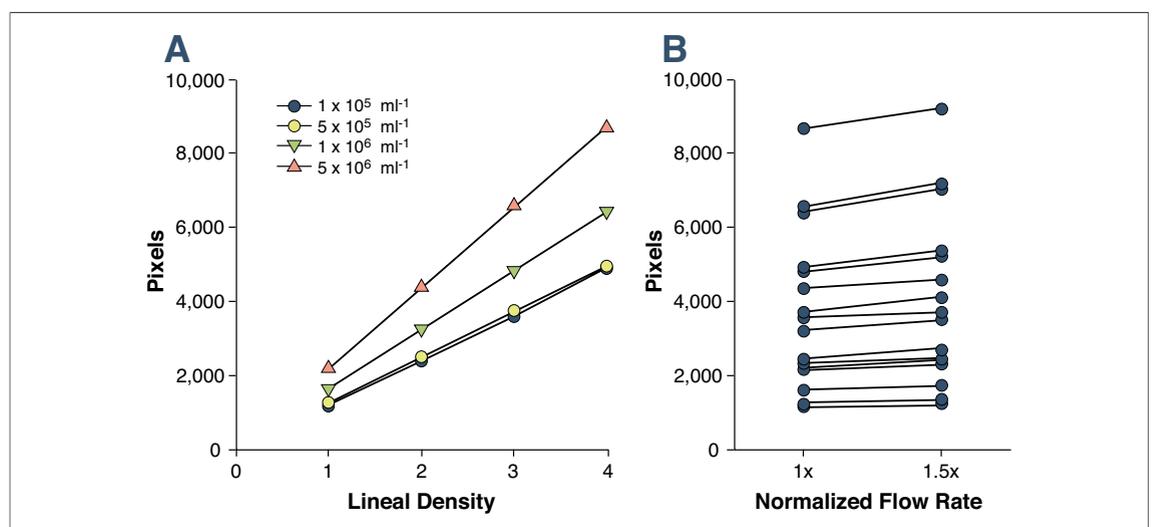
Figure 2. In Vitro Validation of Linear Density

(A) Area of enhancement on contrast-enhanced ultrasound with maximum intensity projection processing during the sequential addition of perfused microtubes (n = 1 to 4). Data are shown for microbubble concentrations varying from 1×10^5 to 5×10^6. **(B)** Area enhancement at baseline (1.0×) and after a 50% increase (1.5×) in flow rate, corresponding to 10 to 15 μl/s per microtube. Data represent the full range of linear densities and microbubble concentrations.

vascular density was almost 3-fold greater in blood-exposed compared with saline-exposed vessels (201 ± 11 vessels vs. 76 ± 10 vessels per section, p < 0.05) (Fig. 4).

In the rabbit femoral artery, a mural inflammatory response 48 h after blood injection was confirmed by both histology and molecular imaging of ICAM-1 (Fig. 5). On CEU with MIP processing performed 1 and 2 weeks after injection, VV functional density was greater for blood-injected vessels compared with either saline-injected or untreated contralateral control arteries (Fig. 6). At these time intervals, there was also a trend toward higher VV blood volume in saline-injected compared with contralateral control vessels, although this did not reach statistical significance after correction for multiple comparisons. Examples of CEU MIP imaging video clips are provided in Online Videos 3 and 4. By 6 weeks, the VV blood volume decreased to the level of control conditions (Fig. 6).

DISCUSSION

The development of methods that can noninvasively quantify VV and plaque neovessels in vivo will have a positive impact on clinical research and probably therapeutic decision making in patients. CEU is one technique that has been used to evaluate plaque neovessels. Most studies have simply used qualitative scoring of the presence of carotid microvessels with microbubble flux (10–13). Quantitative assessment using traditional CEU perfusion imaging methods is possible but may not be well suited for quantifying progression or regression of the VV for several reasons. First, functional vascular density rather than microvascular flow may be a better measure of risk because the detrimental effects of plaque neovascularization are more likely to depend simply on the density of functional microvessels rather than on the flow rate through them. An index of blood volume can be measured with CEU using the plateau value of post-destruction refill kinetics (18). However, this value is influenced by microbubble concentration in the blood pool, which varies over time and between subjects. Absolute blood volume can be calculated by normalization to blood pool, but for VV imaging, this process is complicated because of the high concentrations of contrast required to detect VV that result in a blood pool signal above the saturation point of the dynamic range.
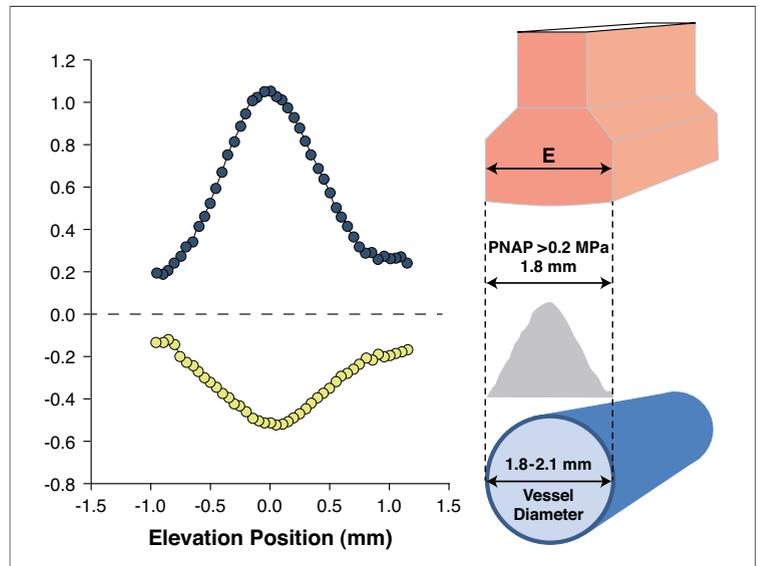
Figure 3. Acoustic Pressure Profile of the Imaging Probe

The graph depicts the peak positive (**blue circles**) and negative (**yellow circles**) acoustic pressure in the elevational (E) dimension. Schematically illustrated at right is the dimension of the rabbit femoral artery in relation to the peak negative acoustic pressure (PNAP) for pressures greater than −0.2 MPa in the elevational dimension when imaging the vessel in the long axis.

Although the degree of plaque enhancement on CEU in previous studies has correlated with the extent of plaque neovascularization on histology, the absolute degree of contrast enhancement can be quite low compared with the morphologic vascular density (10,11,13). In nonhuman primates with atherosclerosis, absolute blood flow in the coronary artery intima-media microcirculation is generally
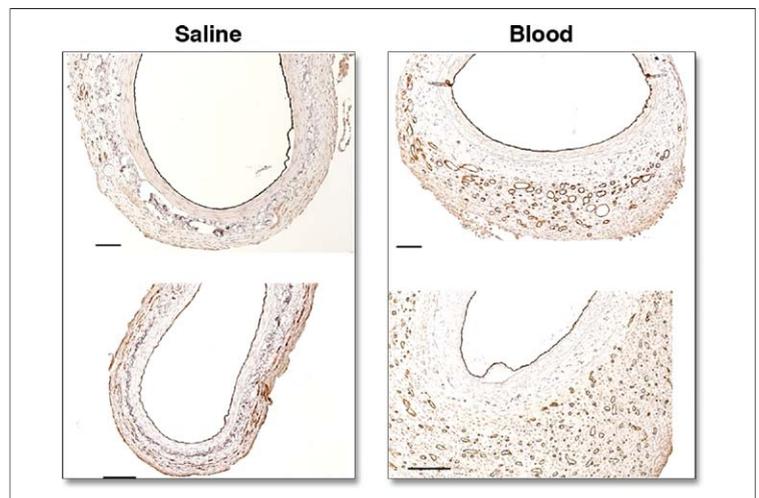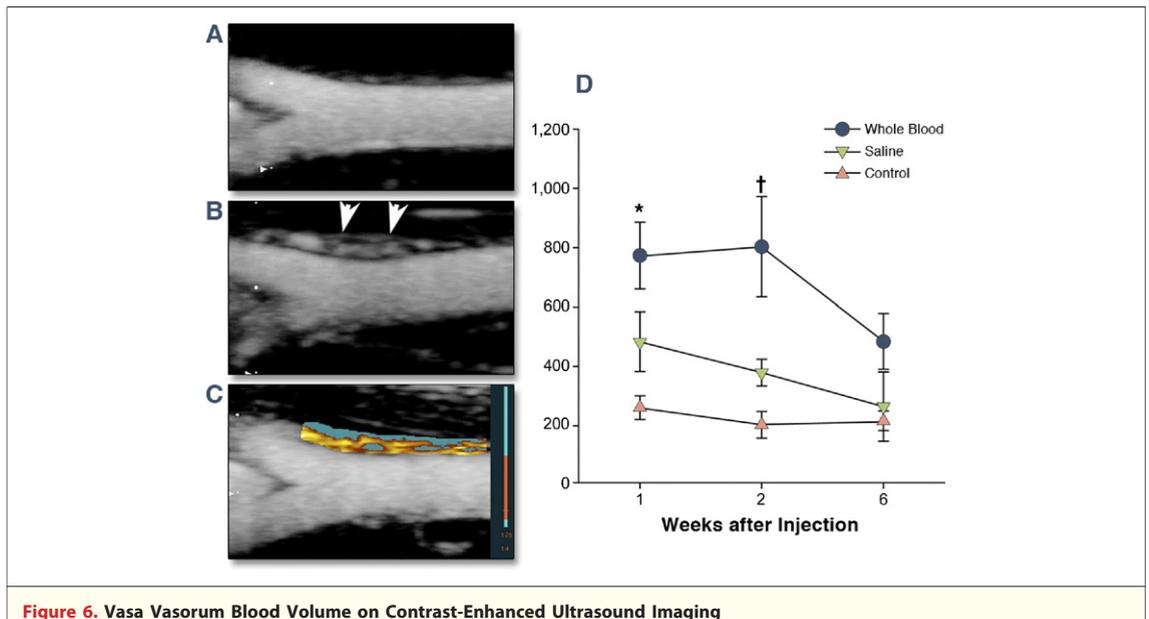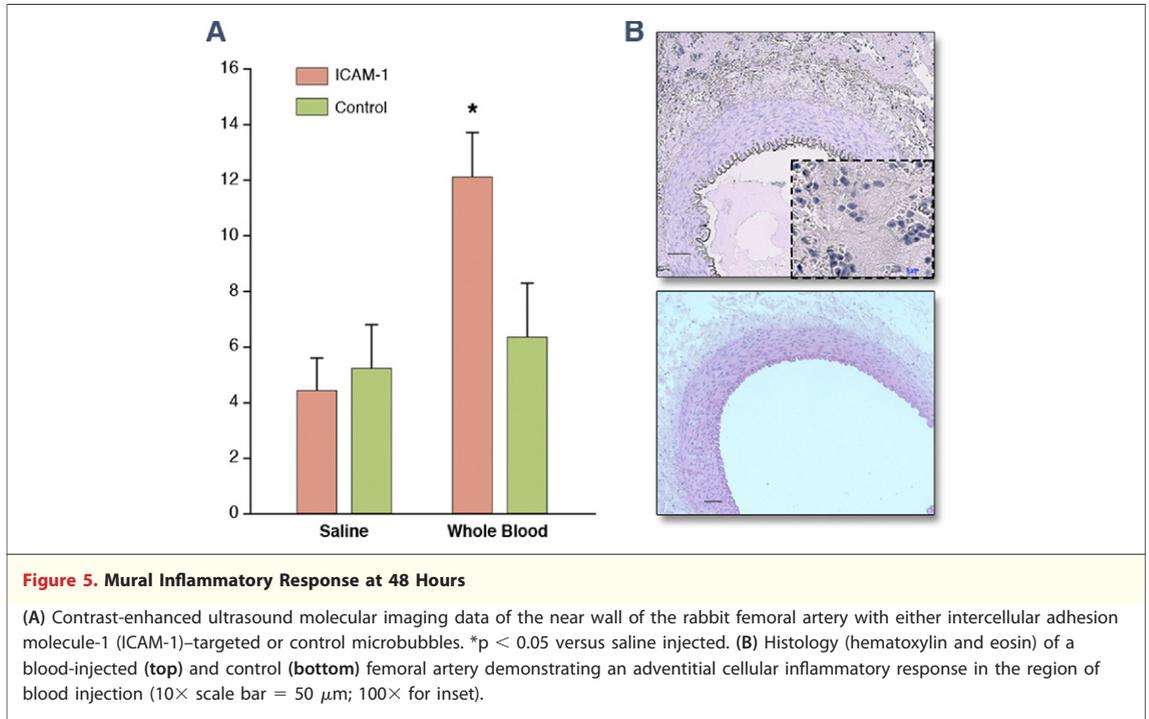
Figure 4. Vasa Vasorum in Blood-Exposed Rat Femoral Artery

Immunohistochemistry for CD31 illustrating marked proliferation of the vasa vasorum 10 days after placement of a cuff containing autologous blood or saline (control subjects). Images represent 2 separate animals from each exposure group. Scale bar = 100 μm.

Figure 5. Mural Inflammatory Response at 48 Hours

(A) Contrast-enhanced ultrasound molecular imaging data of the near wall of the rabbit femoral artery with either intercellular adhesion molecule-1 (ICAM-1)–targeted or control microbubbles. *p < 0.05 versus saline injected. (B) Histology (hematoxylin and eosin) of a blood-injected (top) and control (bottom) femoral artery demonstrating an adventitial cellular inflammatory response in the region of blood injection (10× scale bar = 50 μm; 100× for inset).

Figure 6. Vasa Vasorum Blood Volume on Contrast-Enhanced Ultrasound Imaging

Examples of maximum intensity projection images 2 s after the destructive pulse sequence are shown for femoral arteries 2 weeks after injection of either saline (A) or whole blood (B), illustrating a greater vasa vasorum (VV) density (arrows) in the latter. (C) Example of pixel intensity threshold analysis for the blood-injected vessel whereby pixels within the region of interest that enhance beyond threshold intensity are displayed in red-orange color scale and those that do not are displayed in blue. (D) Mean (± standard error of the mean) area of enhancement on pixel intensity threshold analysis, an index of functional VV blood density. Data for contralateral noninjected control vessels were similar between treatment cohorts and are grouped. *p < 0.05 versus control contralateral artery; †p < 0.05 versus both contralateral and saline-injected arteries (corrected for multiple comparisons).

<0.2 ml/min/g (19). Hence, plaque neovessels in atherosclerosis are similar to neovessels in certain tumors where the proportion of vessels that have active flow at any time is low.

Because of these issues, we used MIP processing of CEU data to enhance sensitivity for detecting microvessels that may have a low functional proportion. MIP detects microvascular linear density by tracking the entire course of microbubble transit through a microvessel and provides a sum of all vessels with any flux during the acquisition period. This technique has an advantage over conventional methods of normalizing vessel wall signal to blood pool signal because 1) it provides higher average intensities that are less affected by noise; 2) data are less influenced by microbubble concentration, thereby obviating the need to normalize to blood pool; and 3) the calculation of the number of pixels that enhance on MIP is less dependent on the size of the region of interest than the measurement of mean contrast intensity.

In this study, simulated vessel "hemorrhage" was used to promote VV proliferation. Our molecular imaging and histology data at 48 h confirmed an inflammatory response in the adventitia that is thought to be one of the primary factors responsible for VV remodeling (3,6). Although a rat model was required to confidently identify blood-induced neovascularization by immunohistology, we could still detect the presence of vessels on histology in the rabbit femoral artery adventitia at 2 weeks. On CEU we detected a marked increase in VV functional density for several weeks after hemorrhage. The increase in VV was transient, probably because of an insufficient environment to maintain neovascularization (possibly from lack of tissue hypoxia in the absence of lesion formation).

Study limitations. There are several other limitations of this study. We created a hyperlipidemic milieu, which is important for promoting a proangiogenic state. However, we did not create focal atherosclerotic plaque per se. We did not correlate CEU MIP with histology data in the rabbit, not only because of limitations in immunohistochemistry but also because of the marked spatial heterogeneity of VV on CEU MIP, which precluded accurate registration to histology. It should also be noted that we relied on volume averaging into a 2-dimensional sector, whereas future use of 3-dimensional imaging could provide more accurate data.

CONCLUSIONS

CEU with MIP processing is a robust method for evaluating VV functional density that is relatively independent of contrast dose. This technique is able to detect temporal changes in VV density in models of mural inflammation.

Reprint requests and correspondence: Dr. Jonathan R. Lindner, Cardiovascular Division, UHN-62, Oregon Health & Science University, 3181 SW Sam Jackson Park Road, Portland, Oregon 97239. *E-mail: lindnerj@ohsu.edu.*

REFERENCES

1. Virmani R, Kolodgie FD, Burke AP, et al. Atherosclerotic plaque progression and vulnerability to rupture: angiogenesis as a source of intraplaque hemorrhage. Arterioscler Thromb Vasc Biol 2005;25:2054-61.

2. Moulton KS, Vakili K, Zurakowski D, et al. Inhibition of plaque neovascularization reduces macrophage accumulation and progression of advanced atherosclerosis. Proc Natl Acad Sci U S A 2003;100:4736-41.

3. Kolodgie FD, Gold HK, Burke AP, et al. Intraplaque hemorrhage and progression of coronary atheroma. N Engl J Med 2003;349:2316-25.

4. Moreno PR, Purushothaman KR, Sirol M, Levy AP, Fuster V. Neovascularization in human atherosclerosis. Circulation 2006;113:2245-52.

5. Sluimer JC, Gasc JM, van Wanroij JL, et al. Hypoxia, hypoxia-inducible transcription factor, and macrophages in human atherosclerotic plaques are correlated with intraplaque angiogenesis. J Am Coll Cardiol 2008;51: 1258-65.

6. Kockx MM, Cromheeke KM, Knaapen MW, et al. Phagocytosis and macrophage activation associated with hemorrhagic microvessels in human atherosclerosis. Arterioscler Thromb Vasc Biol 2003;23:440-6.

7. Takano M, Mizuno K, Okamatsu K, Yokoyama S, Ohba T, Sakai S. Mechanical and structural characteristics of vulnerable plaques: analysis by coronary angioscopy and intravascular ultrasound. J Am Coll Cardiol 2001;38: 99-104.

8. Takaya N, Yuan C, Chu B, et al. Presence of intraplaque hemorrhage stimulates progression of carotid atherosclerotic plaques: a high resolution magnetic resonance imaging study. Circulation 2005;111:2768-75.

9. Underhill HR, Yuan C, Yarnykh VL, et al. Arterial remodeling in the sub-clinical carotid artery disease. J Am Coll Cardiol Img 2009;2:1381-9.

10. Shah F, Balan P, Weinberg M, et al. Contrast-enhanced ultrasound imaging of atherosclerotic carotid plaque neovascularization: a new surrogate marker of atherosclerosis? Vasc Med 2007;12:291-7.

11. Feinstein SB. Contrast ultrasound imaging of the carotid artery vasa vasorum and atherosclerotic plaque neovascularization. J Am Coll Cardiol 2006;48:236-43.

12. Vicenzini E, Giannoni MF, Puccinelli F, et al. Detection of carotid adventitial vasa vasorum and plaque vascularization with ultrasound cadence contrast pulse sequencing technique and echo-contrast agent. Stroke 2007;38: 2841-3.

13. Coli S, Magnoni M, Sangiorgi G, et al. Contrast-enhanced ultrasound imaging of intraplaque neovascularization in carotid arteries. J Am Coll Cardiol 2008;52:223-30.

14. Pascotto M, Leong-Poi H, Lankford M, et al. Assessment of ischemia-induced microvascular remodeling using contrast-enhanced ultrasound vascular anatomic mapping. J Am Soc Echocardiogr 2007;20:1100–8.

15. Micari A, Sklenar J, Belcik JT, Kaul S, Lindner JR. Automated detection of the spatial extent of perfusion defects and viability on myocardial contrast echocardiography. J Am Soc Echocardiogr 2006;19:379–85.

16. Kaufmann BA, Carr CL, Belcik JT, et al. Molecular imaging of the initial inflammatory response in atherosclerosis: implications for early detection of disease. Arterioscler Thromb Vasc Biol 2010;30:54–9.

17. Sakar K, Shi WT, Chatterjee D, Forsberg F. Characterization of ultrasound contrast microbubbles using in vitro experiments and viscous and viscoelastic interface models for encapsulation. J Acoust Soc Am 2000;108:539–50.

18. Wei K, Jayaweera AR, Firoozan S, Linka A, Skyba DM, Kaul S. Quantification of myocardial blood flow with ultrasound induced destruction of microbubbles administered as a constant venous infusion. Circulation 1998;97:473–83.

19. Heistad DD, Armstrong ML. Blood flow through vasa vasorum of coronary arteries in atherosclerotic monkeys. Arteriosclerosis 1986;6:326–31.

Key Words: contrast ultrasound ■ microbubbles ■ plaque hemorrhage ■ vasa vasorum.

⊞ APPENDIX

For supplemental videos and their legends, please see the online version of this article.